Electronic Supplementary Information (ESI)

A New 3D Luminescent Ba-Organic Framework with High Open Metal Sites: CO_2 Fixation, Luminescent Sensing and Dye Sorption†

Meng Wang, Jiao Liu, Jing Jin, Dan Wu, Guoping Yang*, Wen-Yan Zhang and Yao-Yu Wang

Key Laboratory of Synthetic and Natural Functional Molecule of the Ministry of Education, Shaanxi Key Laboratory of Physico-Inorganic Chemistry, College of Chemistry & Materials Science, Northwest University, Xi'an 710127, Shaanxi, P. R. China.

E-mail address:*E-mail: ygp@nwu.edu.cn (G. Yang).

Contents

Table S1 Selected bond lengths [Å] and angles [º] for **1**.

1			
Ba(2)-O(11)#1	2.626(5)	O(11)#1-Ba(2)-O(5)#2	109.49(18)
Ba(2)-O(5)#2	2.686(6)	O(11)#1-Ba(2)-O(15)	101.8(2)
Ba(2)-O(15)	2.738(8)	O(5)#2-Ba(2)-O(15)	72.5(2)
Ba(2)-O(9)#3	2.756(5)	O(11)#1-Ba(2)-O(9)#3	164.01(16)
Ba(2)-O(2)#4	2.807(5)	O(5)#2-Ba(2)-O(9)#3	72.89(16)
O(10)-Ba(1)#4	2.692(6)	O(15)-Ba(2)-O(9)#3	94.0(2)
O(10)-Ba(3)#4	3.038(6)	O(11)#1-Ba(2)-O(2)#4	84.36(17)
O(11)-Ba(2)#11	2.626(5)	O(5)#2-Ba(2)-O(2)#4	141.59(19)
O(11)-Ba(1)#12	2.947(5)	O(15)-Ba(2)-O(2)#4	69.6(2)
Ba(2)-O(1)#4	2.848(5)	O(9)#3-Ba(2)-O(2)#4	103.62(17)
Ba(2)-O(4)	2.868(6)	O(11)#1-Ba(2)-O(1)#4	73.57(16)
Ba(2)-O(3)	2.967(6)	O(5)#2-Ba(2)-O(1)#4	171.01(17)
Ba(1)-O(10)#6	2.692(6)	O(15)-Ba(2)-O(1)#4	115.6(2)
Ba(1)-O(1)#5	2.701(5)	O(5)-Ba(3)-O(6)	45.34(17)
Ba(1)-O(13)	2.720(7)	O(14)-Ba(3)-O(6)	131.2(2)
Ba(1)-O(8)	2.740(5)	O(16)-Ba(3)-O(8)	129.5(3)
Ba(1)-O(14)	2.790(7)	O(7)-Ba(3)-O(8)	46.48(16)
Ba(1)-O(11)#8	2.947(5)	O(5)-Ba(3)-O(8)	146.52(19)
Ba(3)-O(3)#9	2.715(6)	O(14)-Ba(3)-O(8)	63.1(2)
Ba(3)-O(16)	2.740(10)	O(6)-Ba(3)-O(8)	124.86(17)
Ba(1)-O(12)#8	2.790(6)	O(16)-Ba(3)-O(10)#6	101.9(3)
Ba(3)-O(9)#6	2.745(5)	O(7)-Ba(3)-O(10)#6	118.56(16)
Ba(3)-O(7)	2.761(5)	O(1)-Ba(1)#7	2.701(5)
Ba(3)-O(5)	2.818(6)	O(1)-Ba(2)#6	2.848(5)
Ba(3)-O(14)	2.838(7)	O(2)-Ba(2)#6	2.807(5)
Ba(3)-O(6)	2.839(6)	O(3)-Ba(3)#2	2.714(6)
Ba(3)-O(8)	2.850(5)	O(4)-Ba(1)#5	2.704(5)
Ba(3)-O(10)#6	3.038(6)	O(5)-Ba(2)#9	2.686(6)
O(9)-Ba(2)#10	2.756(5)	O(9)-Ba(3)#4	2.745(5)

Symmetry transformations used to generate equivalent atoms of **1**: #1 x, y, z+1; #2 -x+1/2, -y+1, z+1/2; #3 -x+1/2, -y, z+1/2; #4 x, y-1, z; #5 -x+1, y-1/2, -z+1/2; #6 x, y+1, z; #7 -x+1, y+1/2, -z+1/2; #8 -x+1, y+1/2, -z-1/2; #9 -x+1/2, -y+1, z-1/2; #10 -x+1/2, -y, z-1/2; #11 x, y, z-1; #12 -x+1, y-1/2, -z-1/2; #13 -x+3/2, -y+1, z+1/2.

Table S2 A comparison of the luminescent MOFs and **1** used for detecting various ions.

MOFs	Quenching constant (K_{sv})/(M^{-1})	Medium	Ref.
	Fe^{3+}		
[Zn(ATA[a])(L)]·H_2O	0.557×10^3	H_2O	1
[Cd(ATA[a])(L)]·$2H_2O$	3.838×10^3	H_2O	1
[Eu_2(TDC[b])$_3$(CH_3OH)$_2$·(CH_3OH)]	3.42×10^3	MeOH	2
FJI-C8[c]	2.188×10^3	DMF	3
Zn-DTA[d]	8.4×10^3	H_2O	4
1	11.7773×10^3	DMF	This work
[Zn(BIPA[e])(tfbdc)]$_n$	1.32×10^{41}	DMF	5
[Cd(BIPA[e])(tfbdc)(H_2O)]·DMF	1.27×10^4	DMF	5
	$Cr_2O_7^{2-}$		
[Cd(ATA[a])(L)]·$2H_2O$	0.97×10^3	H_2O	1
[Zn(ATA[a])(L)]·H_2O	1.485×10^3	H_2O	1
1	9.15788×10^3	DMF	This work
[Zn(BIPA[e])(tfbdc[f])]$_n$	1.77×10^4	DMF	5
[Cd(BIPA[e])(tfbdc[f])(H_2O)]·DMF	1.98×10^4	DMF	5
	CrO_4^{2-}		
[Zn(ATA[a])(L)]·H_2O	2.623×10^3	H_2O	1
[Cd(ATA[a])(L)]·$2H_2O$	3.119×10^3	H_2O	1
1	3.5927×10^3	DMF	This work
[Zn_3(L[g])(OH)(H_2O)$_5$]·NMP·$2H_2O$	1.3×10^4	H_2O	6

ATA[a] = 2-aminoterephthalic acid; TDC [b] = 2,5-thiophenedicarboxylic acid; TDPAT[c] = 2,4,6-tris(3,5-dicarboxylphenylamino)-1,3,5-triazine; DTA[d] = 2,5-di(1*H*-imidazol-1-yl)terephthalic acid; BIPA[e] = bis(4-(1*H*-imidazol-1-yl)phenyl)amine; tfbdc[f] = 2,3,5,6-tetrafluorobenzene -1,4-dicarboxylic acid; L[g] = 2,4-di(3,5-dicarboxylphenyl) benzoic acid.

S1 Materials and Measurements.

All of the reagents and solvents were used directly without further purification, because of they were purchased from commercial sources. The H_3L ligand was obtained from Beijing Inokai Technology Company. The analysis of C, H and N elements were mainly conducted by the Perkin-Elmer 2400 C elemental analyzer. Fourier transform infrared (FT-IR) analysis was carried on an Equinox-55 FT-IR spectrometer with KBr discs in the range of 4000-400 cm^{-1}. Thermogravimetric analyses (TGA) was performed on a NETZSCH STA 449 C microanalyzer analyzer under flowing N_2 with a heating rate of 10 °C min^{-1}. Powder X-ray diffraction (PXRD) data was collected using a Bruker D8 ADVANCE X-ray powder diffractometer equipped with Cu-Kα (λ = 1.5418 Å and 2θ at 5-50°). The luminescence performance data was obtained with Hitachi F4500 fluoresc-ence spectrophotometer at ambient temperature. The X-ray photoelectron spectroscopy (XPS) was performed on an AXIS Ultra spectrometer. The UV-Vis spectra was earned on Hitachi U-3310 spectrometer.

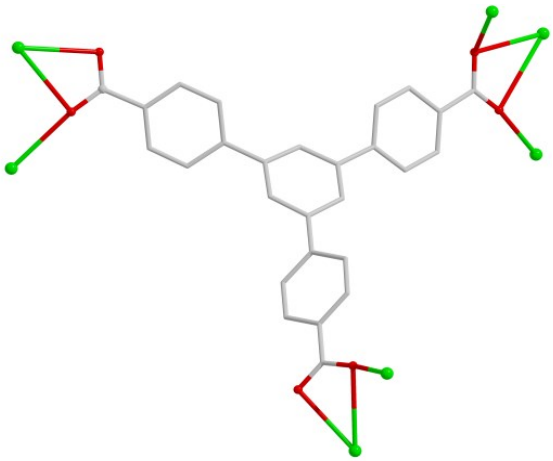

Fig. S1 The coordination modes of L^{3-} ligands in complex **1**.

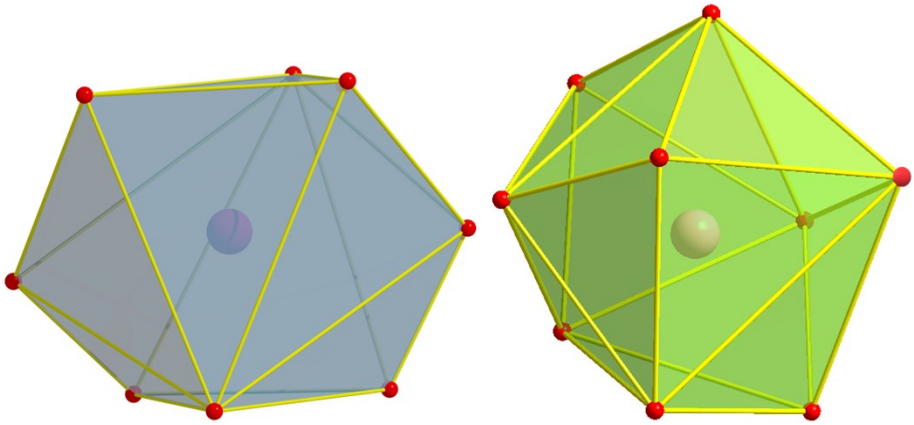

(a) **(b)**

Fig. S2 (a) The distorted dodecahedron of **Ba1** and **Ba2**; (b) A distorted tetrakaidecahedron coordination geometry of **Ba3** of complex **1**.

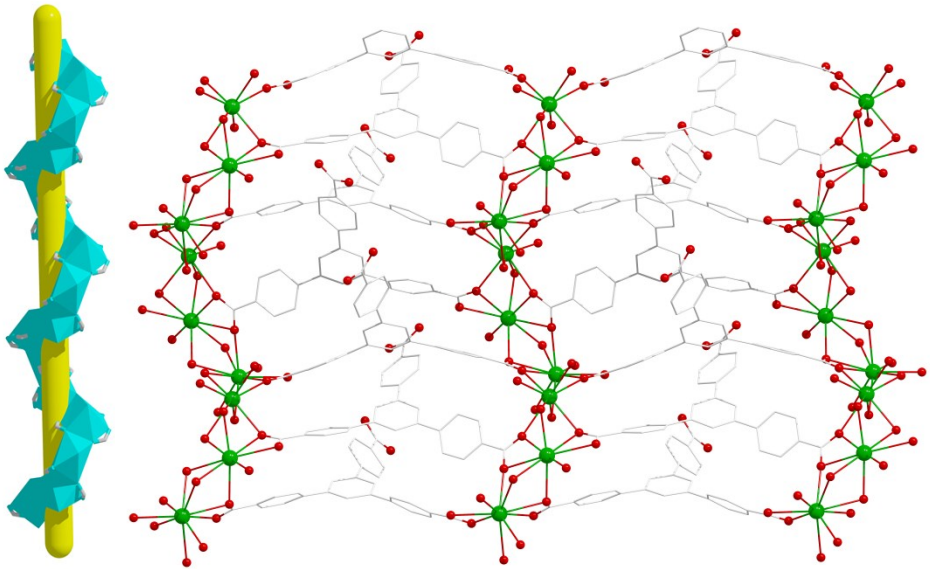

(a) **(b)**

Fig. S3 (a) The helical rod **SBUs** metal chain viewed along the **b** axis; (b) 2D layer structure of complex

1, the coordinated NMP are omitted for clarity.

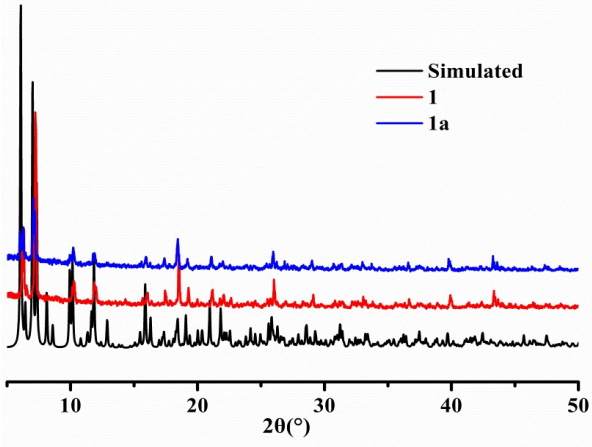

Fig. S4 PXRD patterns of complex **1** and complex **1a**.

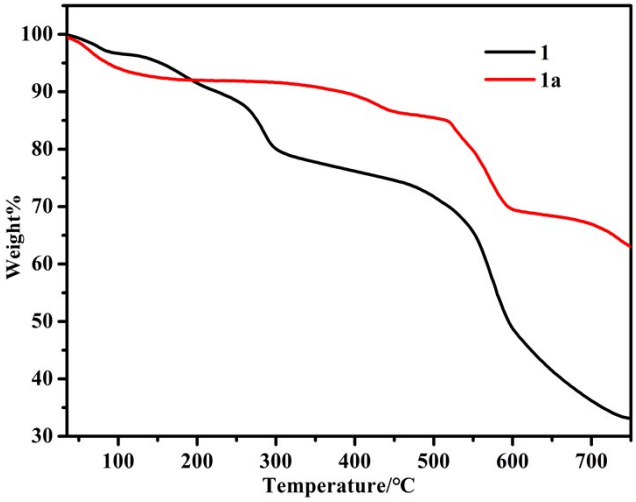

Fig. S5 The TGA curves of complex **1**.

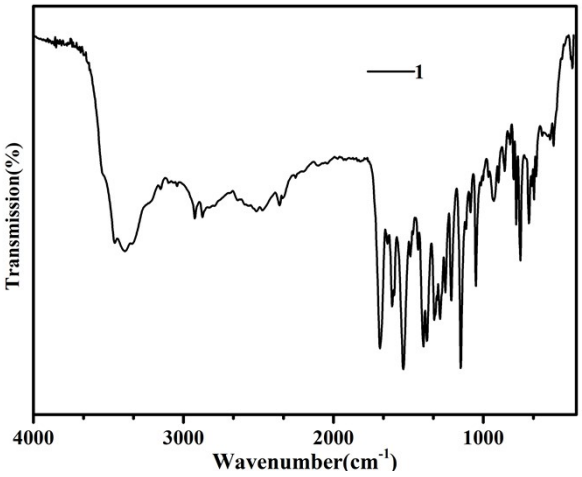

Fig. S6 The FT-IR spectra of complex **1**.

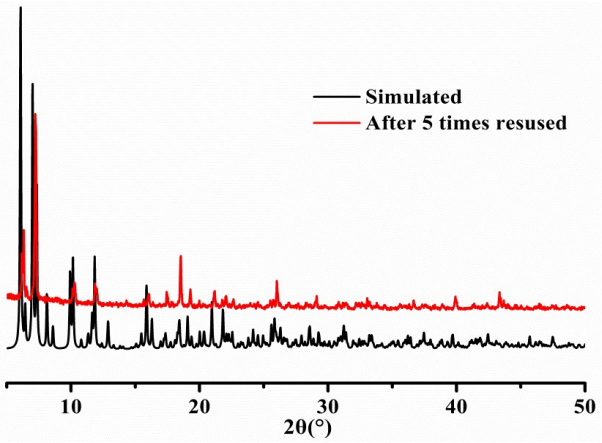

Fig. S7 PXRD pattern after catalytic experiment of complex **1**.

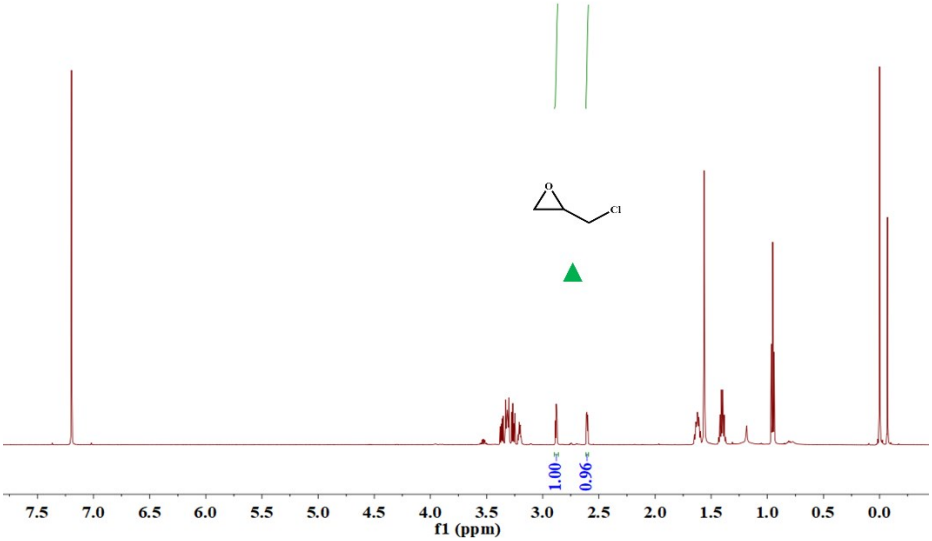

(a) ^{1}H NMR spectrum of epoxide with complex **1a** (Table 2, entry 1).

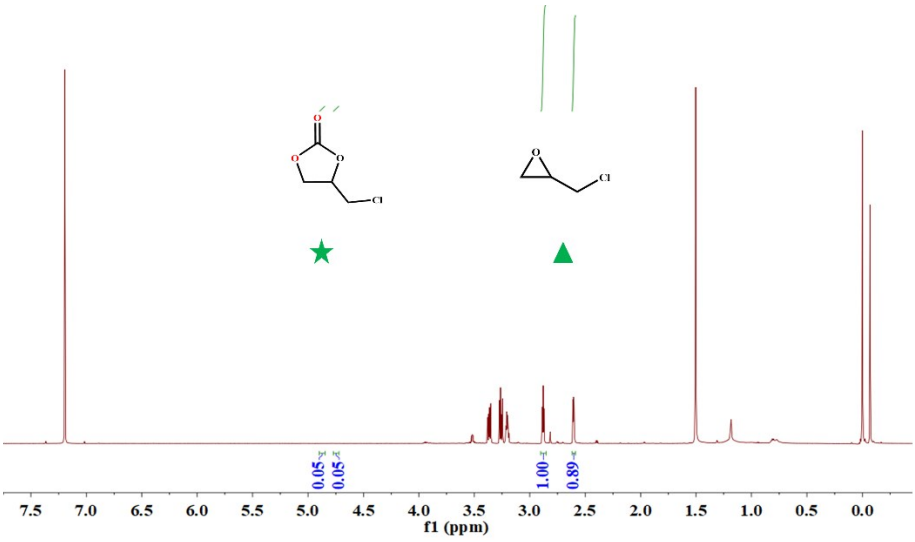

(b) ^{1}H NMR spectrum of cyclic carbonate and epoxide with TBAB (Table 2, entry 2).

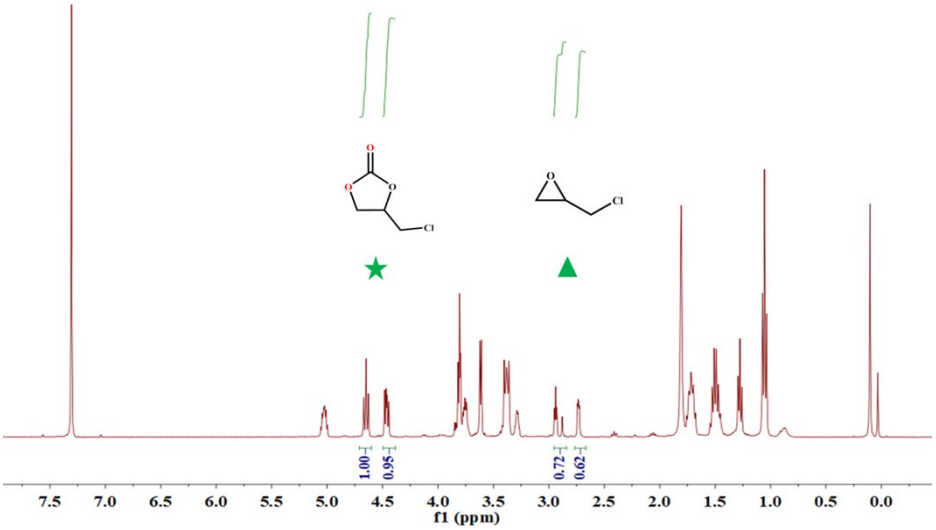

(c) ^{1}H NMR spectrum of cyclic carbonate and epoxide with complex **1a** and TBAB (Table 2, entry 3).

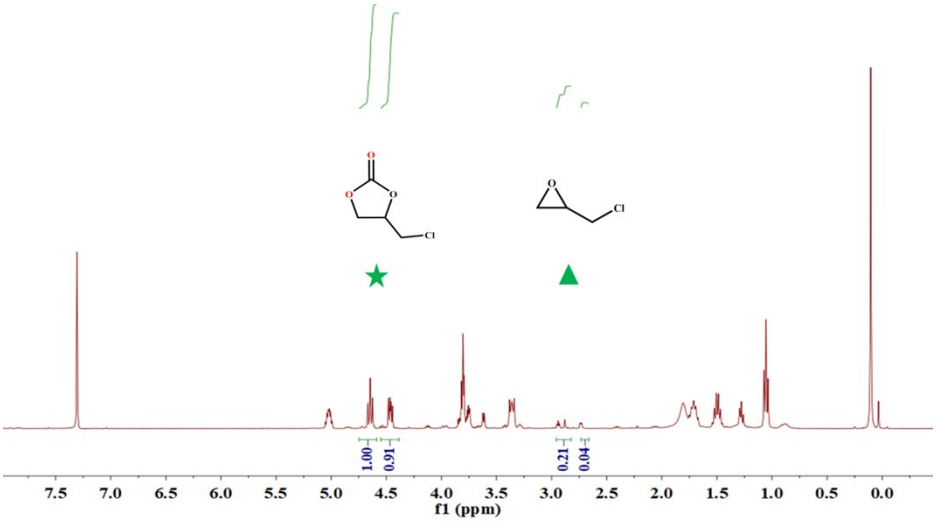

(d) ^{1}H NMR spectrum of cyclic carbonate and epoxide with complex **1a** and TBAB (Table 2, entry 4).

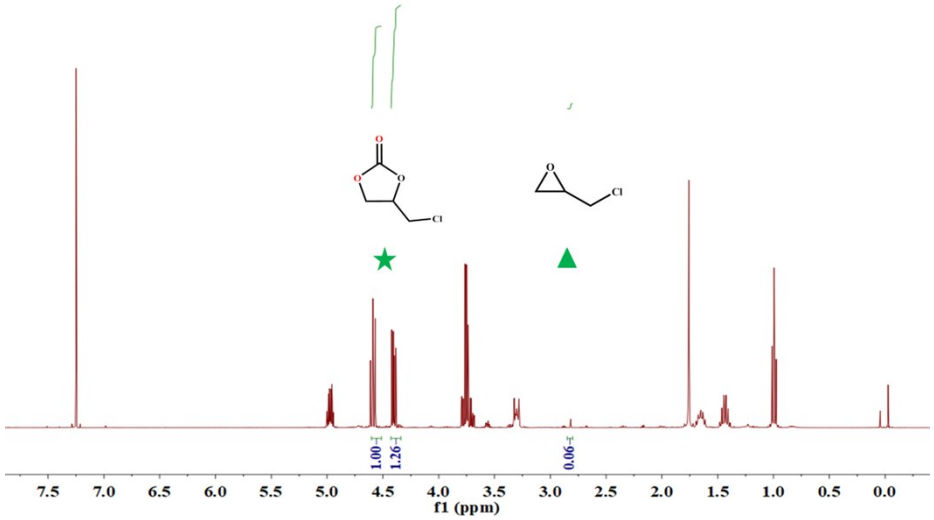

(e) ^{1}H NMR spectrum of cyclic carbonate and epoxide with complex **1a** and TBAB (Table 2, entry 5).

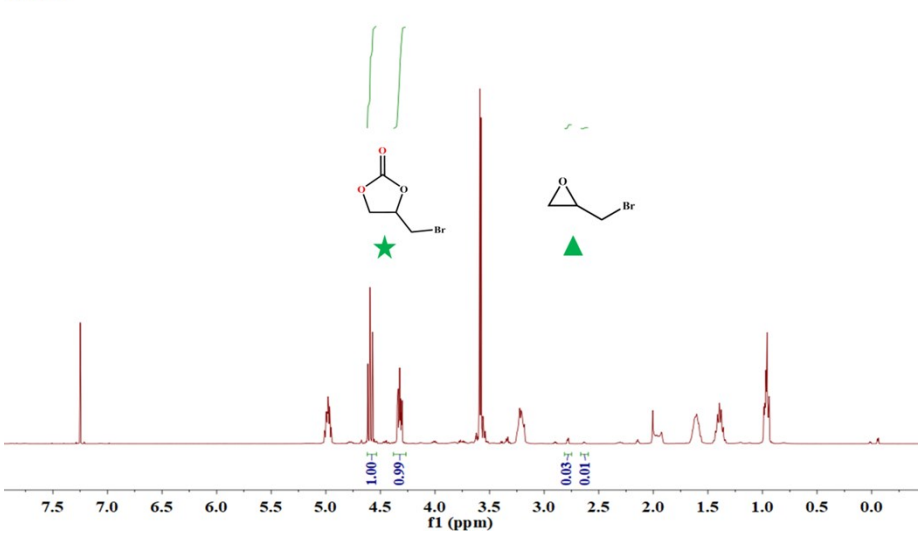

(f) ^{1}H NMR spectrum of cyclic carbonate and epoxide with complex **1a** and TBAB (Table 2, entry 6).

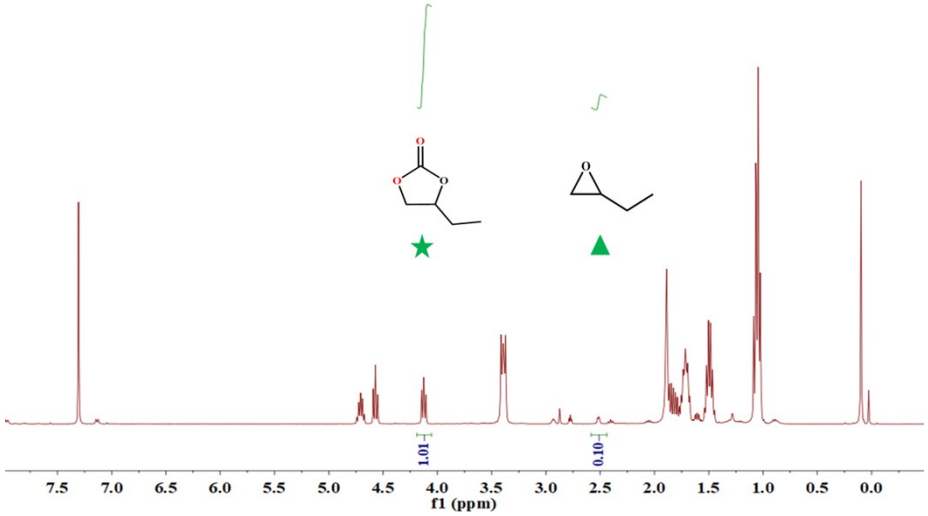

(g) ^{1}H NMR spectrum of cyclic carbonate and epoxide with complex **1a** and TBAB (Table 2, entry 7).

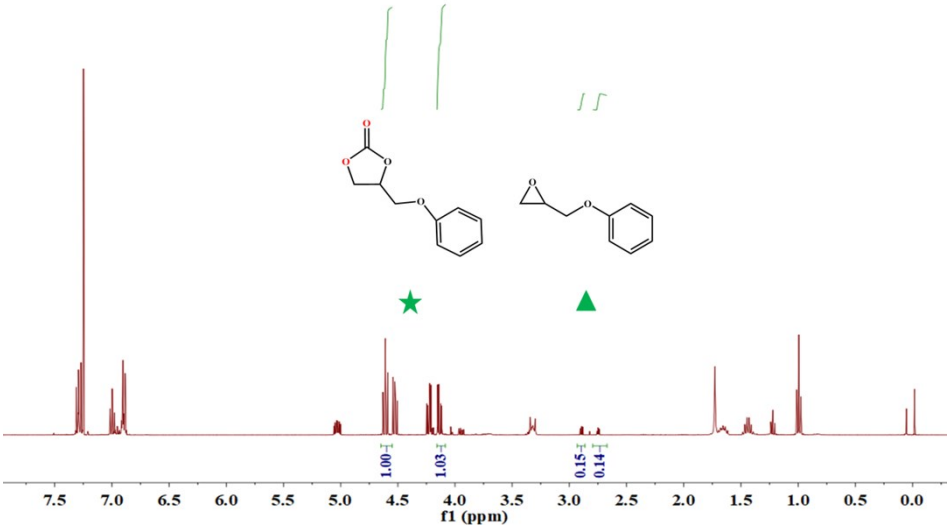

(h) ^{1}H NMR spectrum of cyclic carbonate and epoxide with complex **1a** and TBAB (Table 2, entry 8).

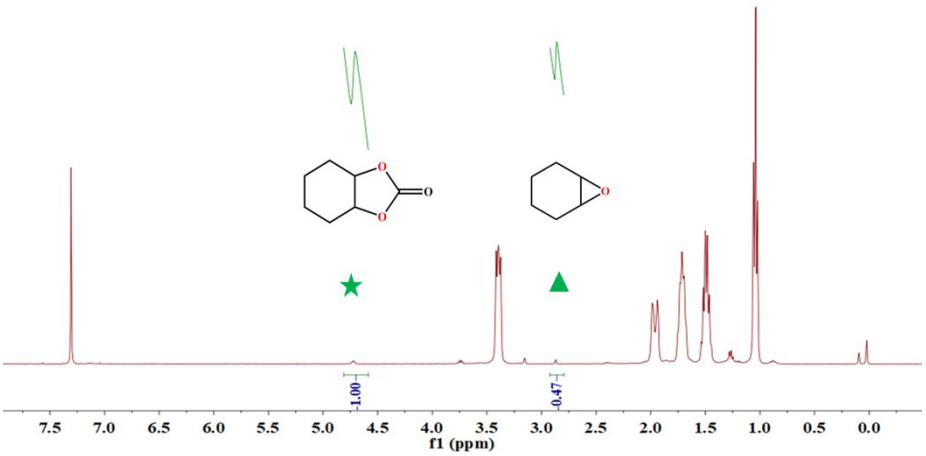

(i) ^{1}H NMR spectrum of cyclic carbonate and epoxide with complex **1a** and TBAB (Table 2, entry 9).

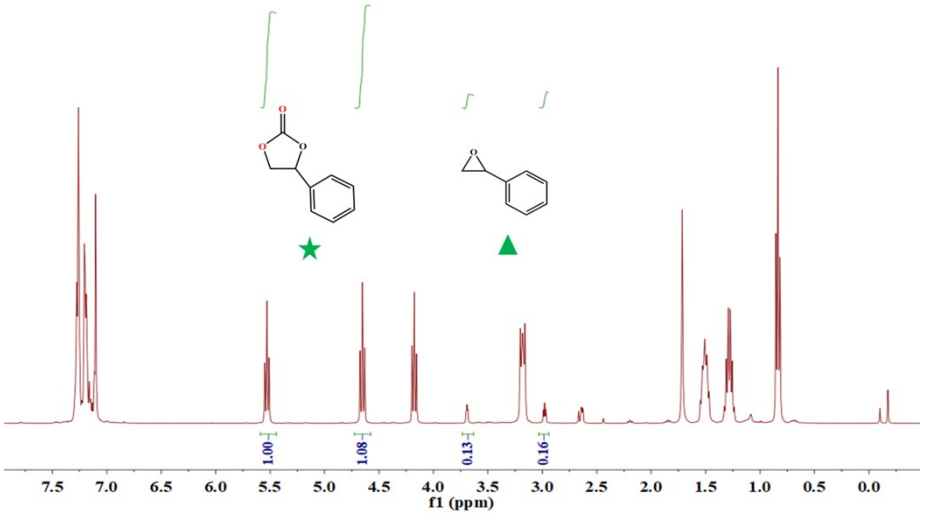

(j) ^{1}H NMR spectrum of cyclic carbonate and epoxide with complex **1a** and TBAB (Table 2, entry 10).

Fig. S8 ^{1}H NMR spectrum of cycloaddition of CO_2 and various epoxide.

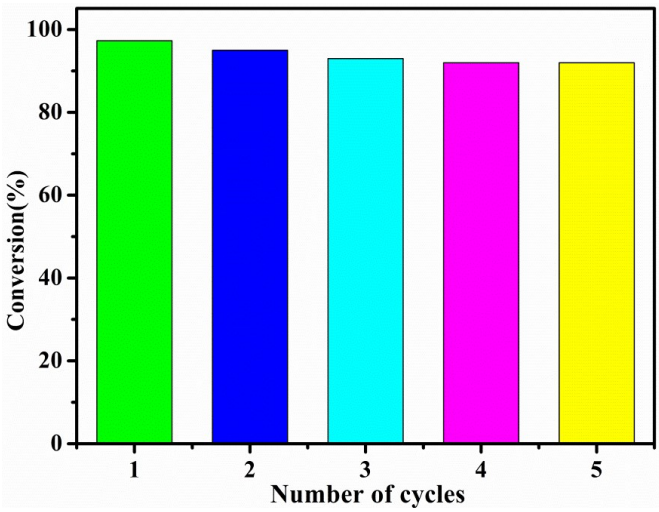

Fig. S9 Cyclic experiments for the cycloaddition CO_2 of complex **1**.

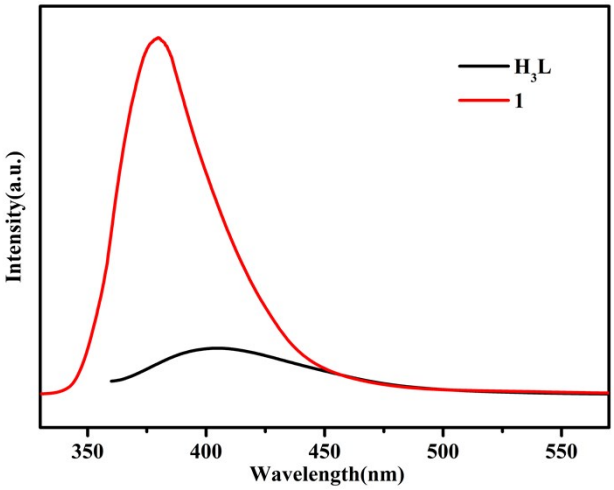

Fig. S10 The solid state emission spectra of free **H_3L** ligand and complex **1**.

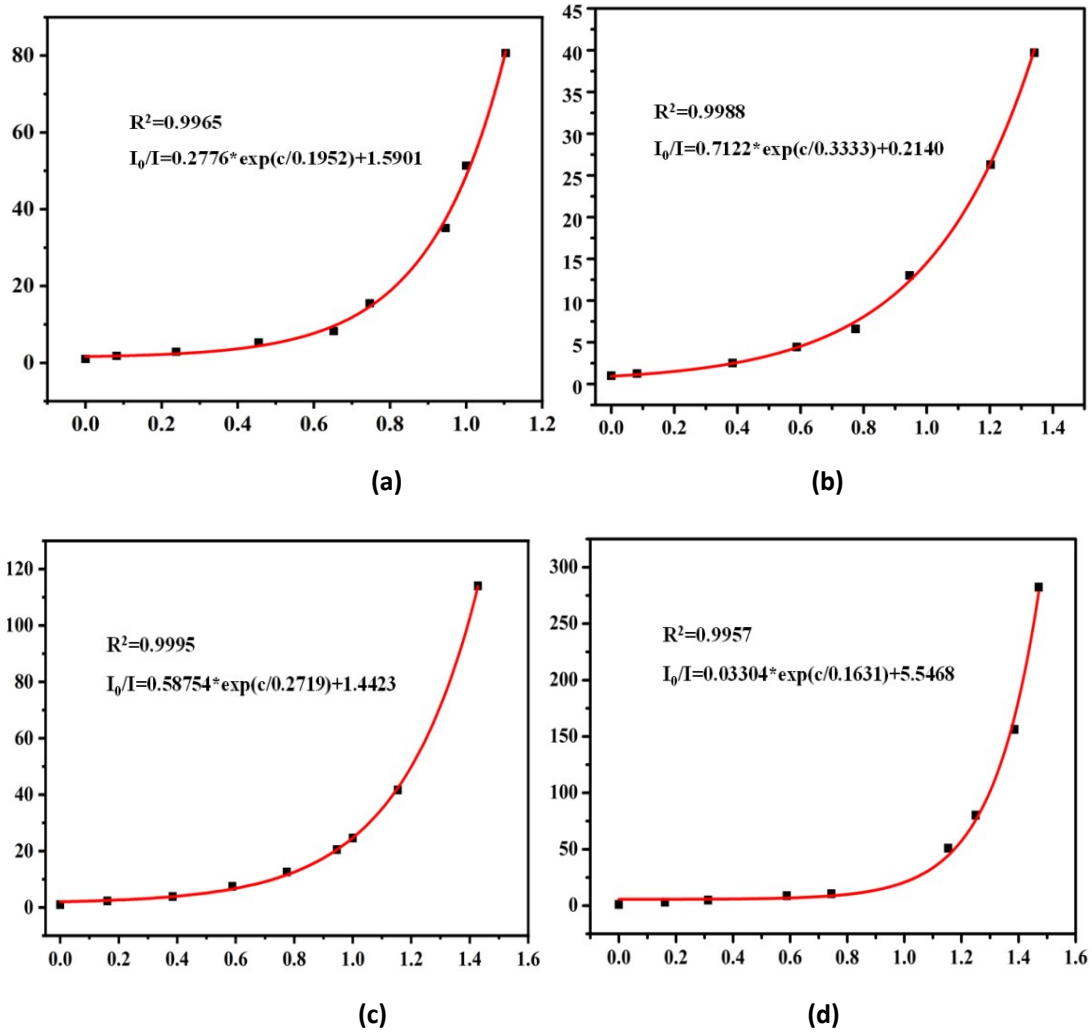

Fig. S11 The relative luminescence intensities of different concentrations Fe^{3+} (a); $Cr_2O_7^{2-}$ (b); CrO_4^{2-} (c) and $[Fe(CN)_6]^{3-}$ (d) @**1** in DMF solutions.

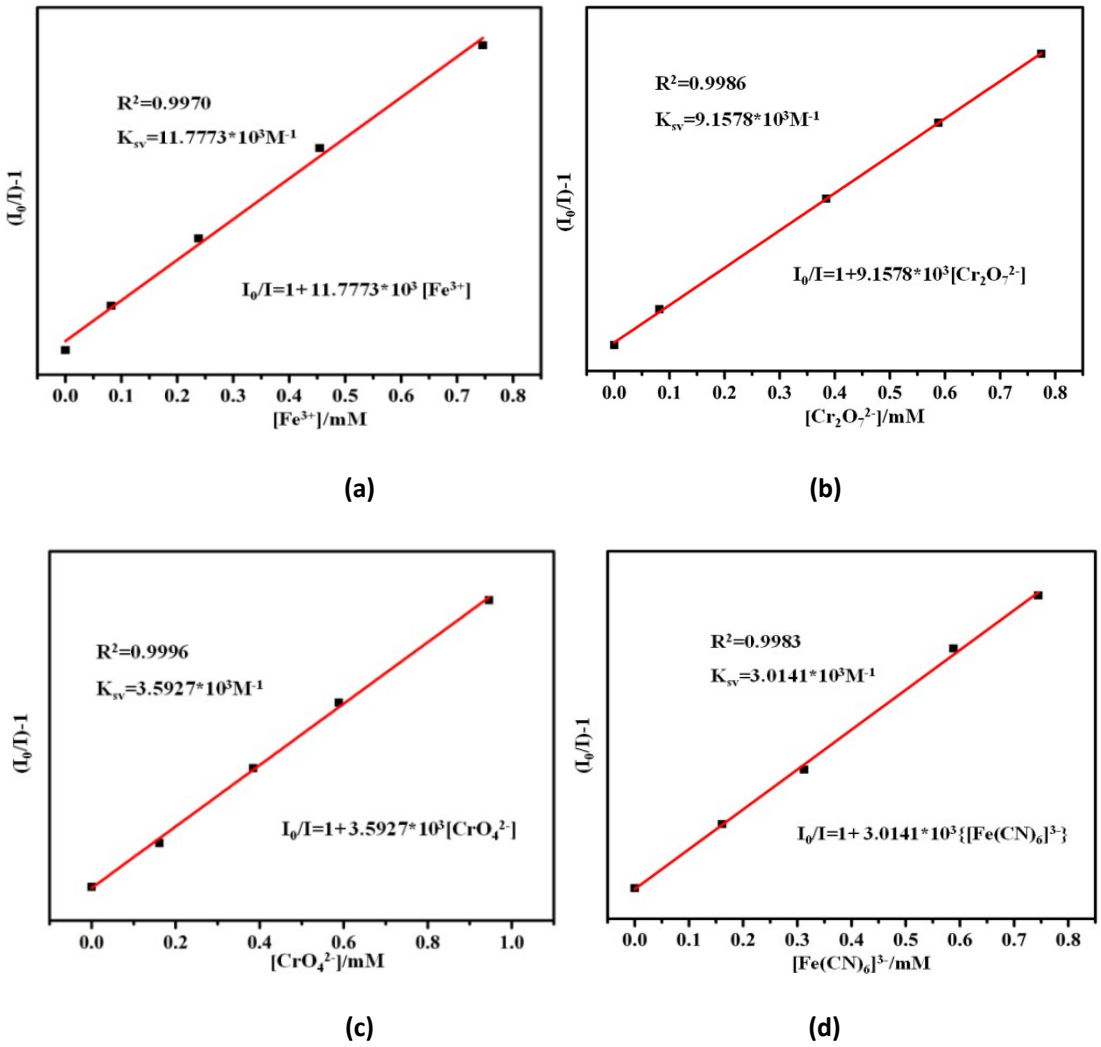

Fig. S12 The linear correlation for the plot of (I_0/I)-1 *vs* concentration of Fe^{3+} (a); $Cr_2O_7^{2-}$ (b); $Cr_2O_4^{2-}$ (c) and $[Fe(CN)_6]^{3-}$ (d) in low concentration range, respectively.

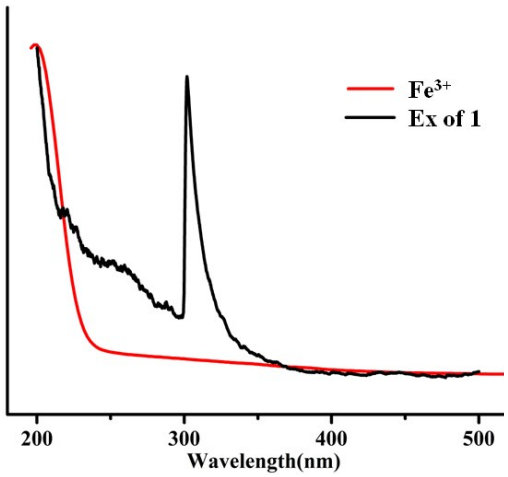

Fig. S13 UV-vis adsorption spectra of various K_x(A) solutions and the excitation spectrum of complex **1**.

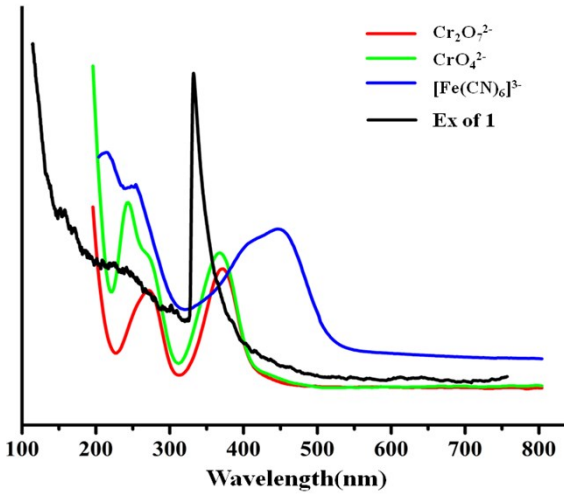

Fig. S14 UV-vis adsorption spectrum of $M(NO_3)_x$ DMF solutions and the excitation spectrum of complex **1** in DMF solution.

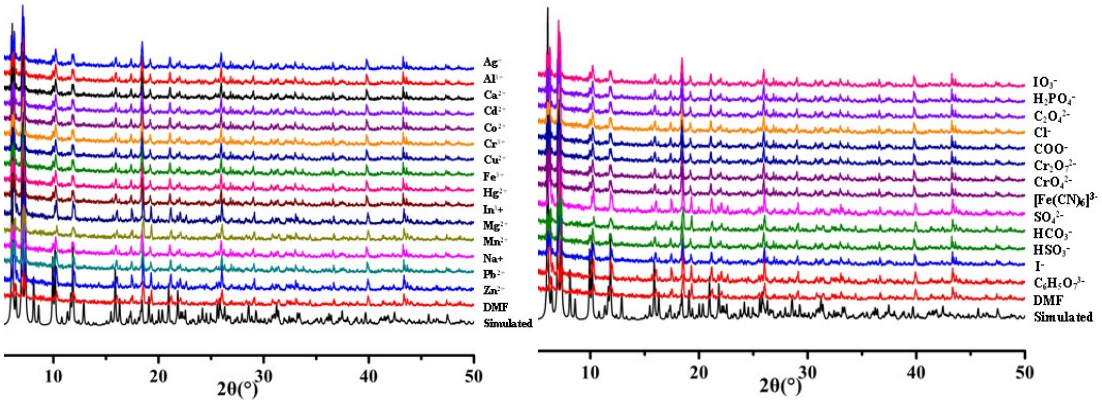

(a) **(b)**

Fig. S15 PXRD patterns of complex **1** treated by different $M(NO_3)_x$ DMF solutions (a) and anion DMF solutions (b).

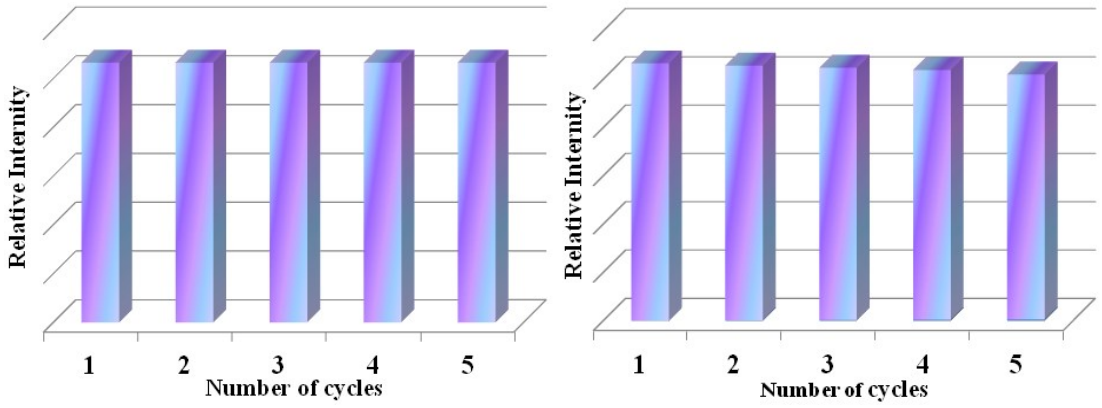

(a) **(b)**

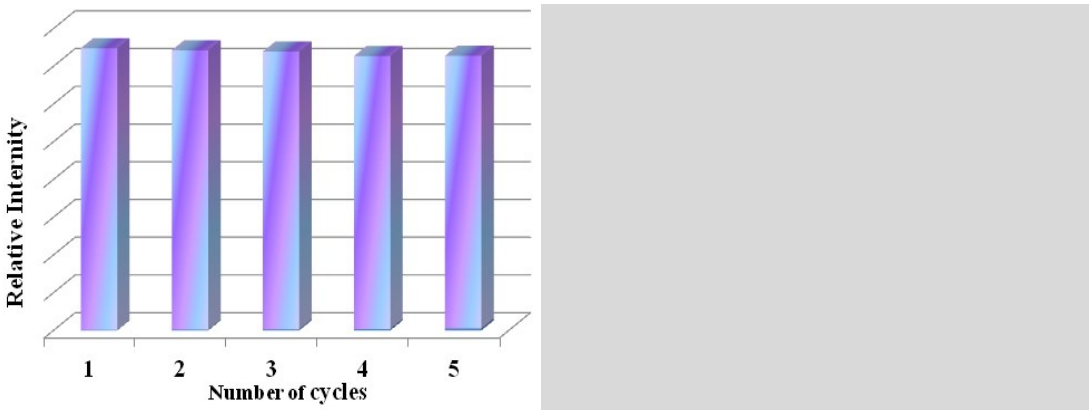

Fig. S16 (a) The fluorescence intensity of complex **1** after five runs sensing experiment with Fe^{3+} (a); $Cr_2O_7^{2-}$ (b); CrO_4^{2-} (c) and $[Fe(CN)_6]^{3-}$ (d).

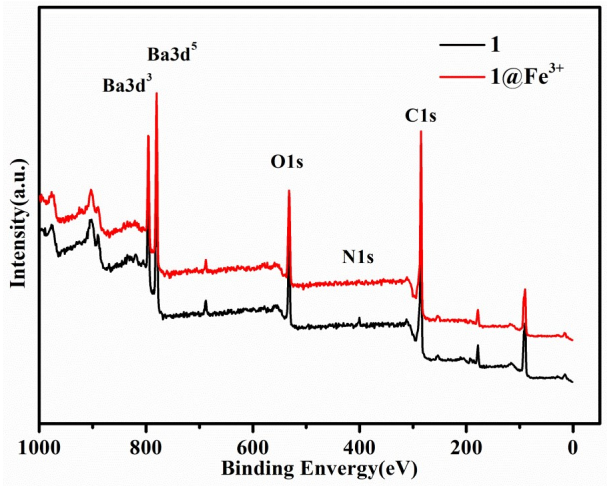

Fig. S17 XPS spectra of **1** (black) and **1**@Fe^{3+} (red).

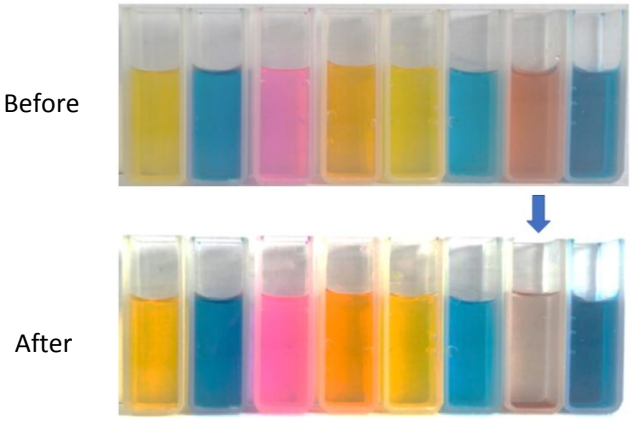

Fig. S18 Color differences of the DMF solutions with complex **1** in various dyes.

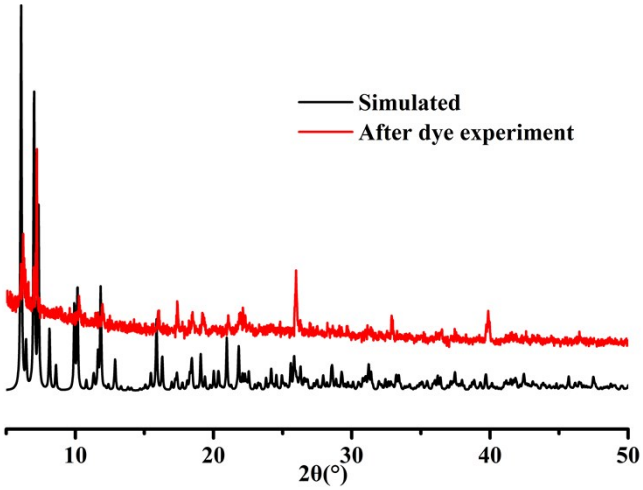

Fig. S19 PXRD pattern after dye experiment of complex **1**.

References

[1] B. Parmar, Y. Rachuri, K. K. Bisht and E. Suresh, *Inorg. Chem.*, 2017, **56**, 10939-10949.

[2] K. Xu, F. Wang, S. Huang, Z. Yu, J. Zhang, J. Yu, H. Gao, Y. Fu, X. Li and Y. Zhao, *RSC Adv.*, 2016, **6**, 91741-91747.

[3] C. H. Chen, X. S. Wang, L. Li, Y. B. Huang and R. Cao, *Dalton Trans.*, 2018, **47**, 3452-3458.

[4] L. Deng, Y. Zhang, D. Zhang, S. Jiao, J. Xu, K. Liu and L. Wang, *CrystEngComm*, 2019, **21**, 6056-6062.

[5] Z. J. Wang, F. Y. Ge, G. H. Sun and H. G. Zheng, *Dalton Trans.*, 2018, **47**, 8257-8263.

[6] Y. T. Yan, J. Liu, G. P. Yang, F. Zhang, Y. K. Fan, W. Y. Zhang, Y. Y. Wang, *CrystEngComm*, 2018, **20** 477-486.